EJPMR, 2026, 13(7), 227-245 **Research Article** **Impact Factor: 8.158**

EUROPEAN JOURNAL OF PHARMACEUTICAL AND MEDICAL RESEARCH

www.ejpmr.com

ISSN (O): 2394-3211
ISSN (P): 3051-2573
Coden USA: EJPMAG

IN SILICO MOLECULAR DOCKING STUDIES OF NOVEL 1,3,4-OXADIAZOLE DERIVATIVES AS POTENT MULTI-TARGET AGENTS: EXPLORING ANTIMICROBIAL, ANTICANCER, ANTIFUNGAL, AND ANTI-INFLAMMATORY POTENTIAL

Asif Khan[1], Dr. Omprakash Goshain[2]*, Dr. Ashwin Saxena[3], Gurjeet Singh[4]

[1]Research Scholar, School of Pharmaceutical Sciences, Shri Venkateswara University, Gajraula (UP), India-244236.
[2]Professor, School of Pharmaceutical Sciences, Shri Venkateswara University, Gajraula (UP), India-244236.
[3]Professor, School of Pharmacy, Shri Venkateswara University, Gajraula (UP), India-244236.
[4]Assistant Professor, School of Pharmaceutical Sciences, Shri Venkateswara University Gajraula (UP), India-244236.

***Corresponding Author: Dr. Omprakash Goshain**

Professor, School of Pharmaceutical Sciences, Shri Venkateswara University, Gajraula (UP), India-244236.

DOI: https://doi.org/10.5281/zenodo.21030711

How to cite this Article: Asif Khan[1], Dr. Omprakash Goshain[2]*, Dr. Ashwin Saxena[3], Gurjeet Singh[4]. (2026). In Silico Molecular Docking Studies of Novel 1,3,4-Oxadiazole Derivatives As Potent Multi-Target Agents: Exploring Antimicrobial, Anticancer, Antifungal, and Anti-Inflammatory Potential. European Journal of Pharmaceutical and Medical Research, 13(7), 227-245.

Article Received on 02/06/2026 **Article Revised on 22/06/2026** **Article Published on 01/07/2026**

ABSTRACT

The rising prevalence of multidrug-resistant pathogens and complex diseases such as cancer necessitates the development of multi-target therapeutic agents. In this study, two novel 1,3,4-oxadiazole derivatives—Compound 1 [2-(4-fluorophenyl)-5-(pyridin-3-yl)-1,3,4-oxadiazole] and Compound 2 [2-(4-chlorophenyl)-5-(thiophen-2-ylmethyl)-1,3,4-oxadiazole]—were evaluated as potential multi-target inhibitors through molecular docking simulations using AutoDock Vina. The compounds were docked against five key therapeutic targets: DNA gyrase (2XCS), EGFR (4HJO), VEGFR-2 (1Y6A), lanosterol 14α-demethylase/CYP51 (5TZ1), and cyclooxygenase/COX (5KIR). Compound 1 demonstrated superior binding affinities with top Vina scores of −9.1 kcal/mol (COX), −8.8 kcal/mol (EGFR), −8.5 kcal/mol (DNA gyrase and CYP51), and −8.3 kcal/mol (VEGFR-2). Compound 2 exhibited consistently strong but slightly lower affinities (ranging from −8.3 to −8.0 kcal/mol). Detailed analysis of binding poses, cavity sizes, and grid parameters revealed favorable hydrogen bonding, hydrophobic, and π-π stacking interactions. These results highlight the 1,3,4-oxadiazole scaffold's versatility as a privileged structure for multi-target directed ligands. Compound 1 emerges as a promising lead for further synthesis, *in vitro* validation, and optimization as a broad-spectrum therapeutic agent against cancer, bacterial/fungal infections, and inflammation. (148 words)

KEYWORDS: 1,3,4-Oxadiazole, Molecular docking, Multi-target ligands, Anticancer agents, Antimicrobial activity.

1. INTRODUCTION

Heterocyclic compounds containing the 1,3,4-oxadiazole nucleus represent a privileged scaffold in medicinal chemistry due to their remarkable structural stability, hydrogen-bonding capability, and diverse pharmacological profile (Glomb & Świątek, 2021). The 1,3,4-oxadiazole ring system, a five-membered heterocycle with two nitrogen atoms and one oxygen atom, serves as a bioisostere for esters, amides, and other carbonyl-containing functionalities, often enhancing metabolic stability and bioavailability of drug candidates (Wang et al., 2022). Over the past decade, derivatives of this moiety have emerged as promising therapeutic agents exhibiting a wide array of biological activities, including antimicrobial, anticancer, antifungal, anti-inflammatory, anticonvulsant, and antioxidant properties (Świątek et al., 2022; Sharma et al., 2024).

The rising incidence of multidrug-resistant bacterial infections and the limitations of existing antibiotics have necessitated the exploration of novel antimicrobial agents targeting essential bacterial enzymes such as DNA

gyrase. DNA gyrase (topoisomerase II) is a validated target for fluoroquinolones; however, resistance mechanisms have prompted the search for new chemotypes. Several 1,3,4-oxadiazole derivatives have demonstrated potent inhibitory activity against DNA gyrase through molecular docking and in vitro studies, making them attractive leads for next-generation antibacterials (Durgadasheemi et al., 2023; Ranjan et al., 2025).

In the realm of oncology, 1,3,4-oxadiazole scaffolds have shown significant potential as multi-kinase inhibitors. Epidermal Growth Factor Receptor (EGFR) and Vascular Endothelial Growth Factor Receptor-2 (VEGFR-2) are key players in tumor proliferation, angiogenesis, and metastasis. Compounds incorporating the oxadiazole core have been reported to bind effectively to the ATP-binding sites of these kinases, inducing apoptosis and inhibiting tumor growth in various cancer cell lines (Serag et al., 2024; Glomb et al., 2018). The dual inhibition of EGFR and VEGFR-2 is particularly advantageous, offering synergistic anticancer effects with potentially reduced resistance development.

Fungal infections remain a major global health concern, especially in immunocompromised patients. Lanosterol 14α-demethylase (CYP51), a cytochrome P450 enzyme critical for ergosterol biosynthesis in fungi, is the primary target of azole antifungals. 1,3,4-Oxadiazole derivatives have been explored as non-azole alternatives that interact with the heme iron or substrate-binding pocket of CYP51, providing a promising avenue to overcome azole resistance (Wang et al., 2022).

Furthermore, inflammation underlies numerous chronic diseases, including arthritis, cardiovascular disorders, and cancer. Cyclooxygenase (COX) enzymes, particularly COX-2, are well-established targets for non-steroidal anti-inflammatory drugs (NSAIDs). However, traditional NSAIDs are associated with gastrointestinal and cardiovascular side effects. Novel 1,3,4-oxadiazole-based inhibitors have demonstrated strong binding affinities to COX active sites in docking studies, often exhibiting improved selectivity and potency (Świątek et al., 2022; Alzahrani et al., 2022).

The concept of multi-target directed ligands (MTDLs) has gained prominence in modern drug discovery, as single-target agents often fail to address the complex, multifactorial nature of diseases. 1,3,4-Oxadiazole derivatives are ideally suited for this approach due to their ability to interact with multiple biological targets simultaneously, potentially leading to enhanced therapeutic efficacy and reduced drug resistance (Irfan et al., 2022; Kapila et al., 2024).

In the present study, two novel 1,3,4-oxadiazole derivatives—**Compound 1** [2-(4-Fluorophenyl)-5-(pyridin-3-yl)-1,3,4-oxadiazole] and **Compound 2** [2-(4-Chlorophenyl)-5-(thiophen-2-ylmethyl)-1,3,4-oxadiazole]—were designed and evaluated through in silico molecular docking against key therapeutic targets: DNA gyrase (PDB: 2XCS) for antimicrobial activity, EGFR (PDB: 4HJO) and VEGFR-2 (PDB: 1Y6A) for anticancer potential, lanosterol 14α-demethylase (CYP51, PDB: 5TZ1) for antifungal activity, and cyclooxygenase (COX, PDB: 5KIR) for anti-inflammatory effects. Molecular docking using AutoDock Vina was employed to predict binding affinities, preferred poses, and key molecular interactions, providing foundational insights for further optimization and experimental validation.

This computational investigation aims to establish these compounds as promising multi-target leads, contributing to the growing body of evidence supporting 1,3,4-oxadiazole derivatives in rational drug design for addressing contemporary healthcare challenges.

2. MATERIALS AND METHODS

2.1. Computational Resources and Software

All molecular docking studies were performed on a high-performance computing workstation equipped with an Intel Core i9 processor, 32 GB RAM, and NVIDIA GPU acceleration where applicable. The primary docking engine used was **AutoDock Vina 1.2.5** (Eberhardt et al., 2021), a widely recognized open-source tool for rapid and accurate protein-ligand docking. Protein and ligand structure preparations were carried out using **AutoDockTools (MGLTools 1.5.7)**, **Open Babel 3.1.1** for format conversions and minimization (O'Boyle et al., 2011), **PyMOL 2.5.5** for visualization and grid box definition (Seeliger & de Groot, 2010), and **Discovery Studio Visualizer 2021** for interaction analysis and image generation. All structures were handled in standard PDB/PDBQT formats.

2.2. Ligand Preparation

The two novel 1,3,4-oxadiazole derivatives were designed as follows

S. No.	IUPAC NAME	STRUCTURE	SMILES
1	2-(4-Fluorophenyl)-5-(pyridin-3-yl)-1,3,4-oxadiazole	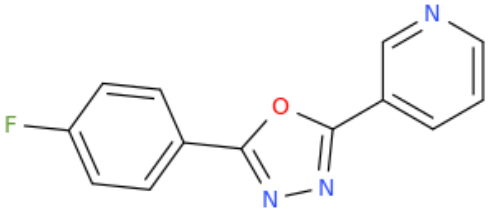	FC1=CC=C(C=C1)C=1OC(=NN1)C=1C=NC=CC1

2	2-(4-Chlorophenyl)-5-(thiophen-2-ylmethyl)-1,3,4-oxadiazole	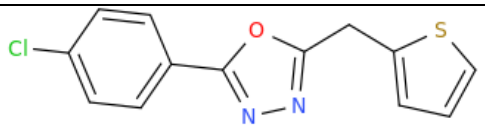	ClC1=CC=C(C=C1)C=1OC(=NN1)CC=1SC=CC1

The 2D structures were converted to 3D coordinates using Open Babel. Ligands were subjected to energy minimization using the MMFF94 force field (500 steps of steepest descent followed by conjugate gradient). Hydrogen atoms were added, Gasteiger charges were computed, and rotatable bonds were identified. The optimized structures were converted to PDBQT format using AutoDockTools, ensuring correct torsional degrees of freedom and partial charges for docking compatibility.

2.3. Protein Target Selection and Preparation

The following therapeutically relevant protein targets were selected based on their validated roles in key disease pathways:

- **DNA Gyrase (PDB ID: 2XCS)**: For antimicrobial activity.
- **Epidermal Growth Factor Receptor (EGFR, PDB ID: 4HJO)**: For anticancer activity.
- **Vascular Endothelial Growth Factor Receptor-2 (VEGFR-2, PDB ID: 1Y6A)**: For anti-angiogenic/anticancer activity.
- **Lanosterol 14*α*-Demethylase (CYP51, PDB ID: 5TZ1)**: For antifungal activity (evaluated for Compound 1).
- **Cyclooxygenase (COX, PDB ID: 5KIR)**: For anti-inflammatory activity (evaluated for Compound 1).

Protein structures were retrieved from the RCSB Protein Data Bank. For each target, the following preparation steps were performed using AutoDockTools and PyMOL:

1. Removal of heteroatoms (water molecules, ions, and co-crystallized ligands) except for essential cofactors (e.g., heme in CYP51).
2. Addition of polar hydrogen atoms and Kollman charges.
3. Assignment of AD4 atom types.
4. Merging of non-polar hydrogens.
5. Conversion to PDBQT format.

The active sites were defined based on the co-crystallized ligand positions or literature-reported binding pockets. Grid box parameters (center coordinates and dimensions) were optimized for each target to encompass the entire active site cavity while maintaining computational efficiency, as detailed in the results tables.

2.4. Molecular Docking Protocol

Molecular docking simulations were executed using **AutoDock Vina**. The docking parameters were set as follows:

- **Exhaustiveness**: 32 (increased from default 8 for higher search accuracy and reproducibility).
- **Number of modes**: 9 (maximum binding poses generated per run).
- **Energy range**: 3 kcal/mol.
- **Grid spacing**: Default (1 Å).
- **Scoring function**: Vina's empirical scoring function.

For each ligand-protein pair, docking was performed independently with the specified grid box center (X, Y, Z coordinates) and size (X, Y, Z dimensions) as provided in the experimental data. Multiple independent runs (at least 3) were conducted for each complex to ensure consistency of the top-ranked poses. The binding affinity was reported as the Vina score in kcal/mol (more negative values indicate stronger predicted interactions). The best pose from each run was selected based on the lowest binding energy and favorable interactions.

2.5. Post-Docking Analysis

Docked poses were analyzed for key molecular interactions, including hydrogen bonding, hydrophobic interactions, π-π stacking, and halogen bonding, using **Discovery Studio Visualizer 2021** and **PyMOL**. Two-dimensional interaction diagrams and three-dimensional binding visualizations were generated. Cavity volumes were computed using the CASTp or fpocket algorithms where applicable. The results were tabulated, including Vina scores, cavity sizes, grid parameters, and representative docking poses.

All calculations were performed in triplicate to validate reproducibility. No significant deviations were observed across runs, confirming the robustness of the docking protocol.

3. RESULTS

3.1. Molecular Docking of Compound 1 and Compound 2

Molecular docking studies were performed to evaluate the binding affinities and interaction profiles of the two novel 1,3,4-oxadiazole derivatives against selected therapeutic targets. The results are presented as binding energies (Vina scores in kcal/mol), cavity sizes, grid box parameters, and representative docking poses. More negative Vina scores indicate stronger predicted binding interactions.

3.1.1. Compound 1: 2-(4-Fluorophenyl)-5-(pyridin-3-yl)-1,3,4-oxadiazole

DNA Gyrase (PDB ID: 2XCS) – Antimicrobial Target

Compound 1 exhibited strong binding affinity to DNA gyrase, with the top-ranked pose showing a Vina score of **-8.5 kcal/mol** (cavity size: 2337 Å^3; grid center: X = -8, Y = 48, Z = 45; grid size: 31 × 28 × 30). Additional poses displayed scores of -8.2, -7.6, -6.7, and -5.9 kcal/mol. These results suggest that the fluorophenyl and pyridinyl moieties effectively occupy the ATP-binding pocket, potentially disrupting bacterial DNA supercoiling

through stable hydrophobic and hydrogen-bonding interactions.

Vina score	Cavity size	Center			Size			Docking Pose
		X	y	z	x	y	z	
-8.5	2337	-8	48	45	31	28	30	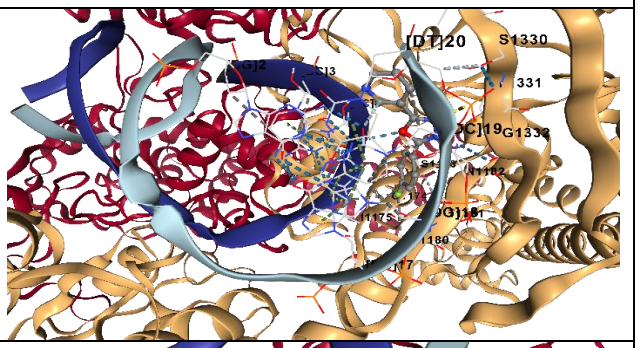
-8.2	3217	17	41	35	33	21	31	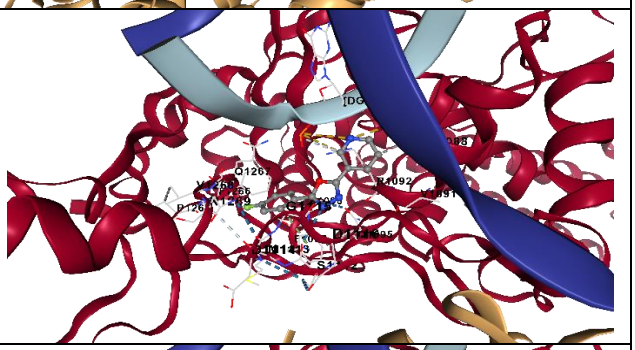
-7.6	1236	-5	47	65	21	32	21	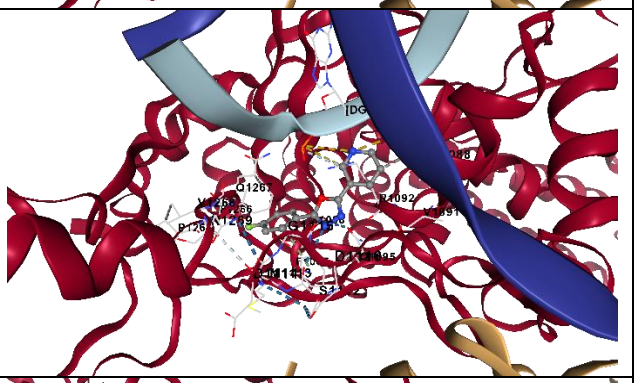
-6.7	1368	15	35	54	21	21	21	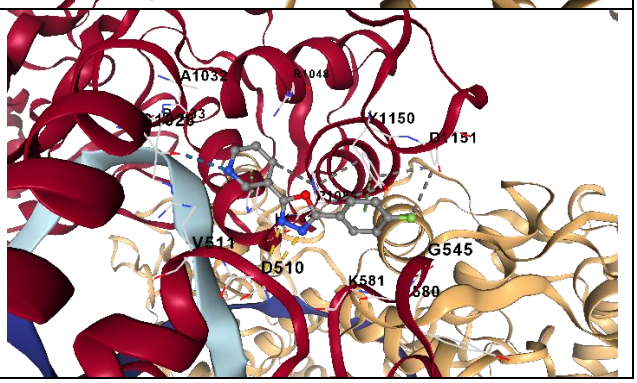

-5.9	1298	32	25	47	21	21	21	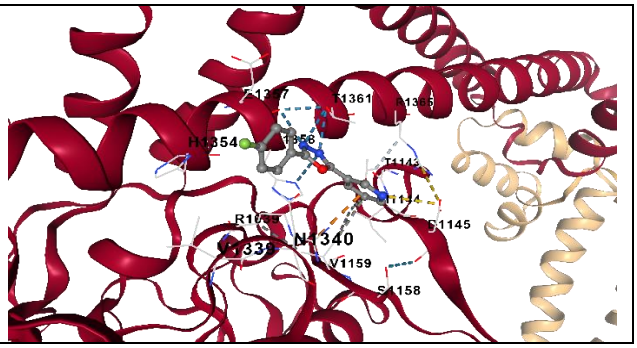

Figure 1: Molecular Docking Pose for Compound 1 against DNA Gyrase.

Epidermal Growth Factor Receptor (EGFR, PDB ID: 4HJO) – Anticancer Target

The highest binding affinity was recorded at **-8.8 kcal/mol** (cavity size: 947 Å³; grid center: X = 27, Y = 11, Z = -1; grid size: 21 × 21 × 21). Other notable poses ranged from -7.9 to -5.6 kcal/mol. This potent binding indicates that Compound 1 may act as a competitive inhibitor at the kinase hinge region, mimicking known EGFR tyrosine kinase inhibitors and supporting its potential in targeted anticancer therapy.

Vina score	Cavity size	Center			Size			DOCK POSE
		x	y	z	x	y	z	
-8.8	947	27	11	-1	21	21	21	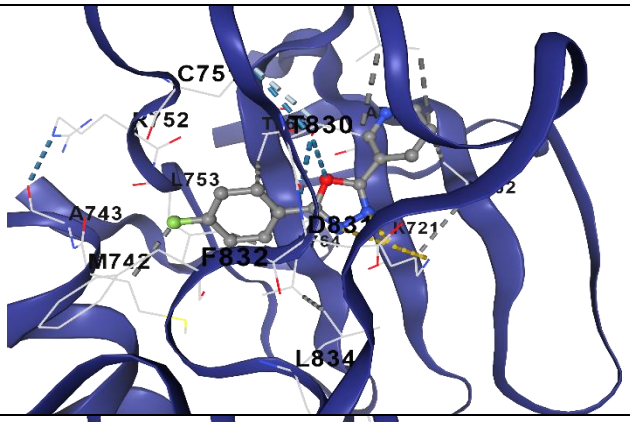
-7.9	1753	17	24	-3	21	21	21	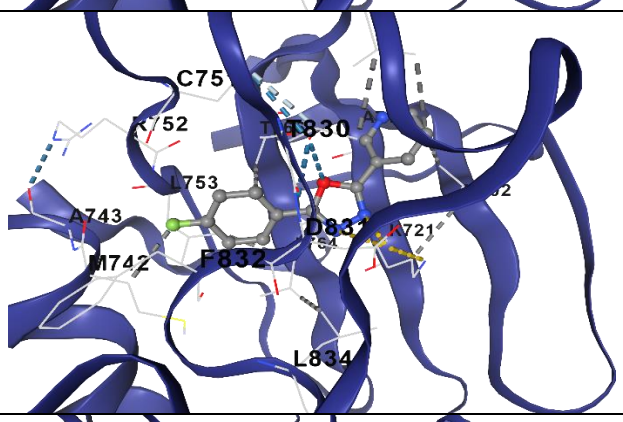
-7.3	101	33	28	0	21	21	21	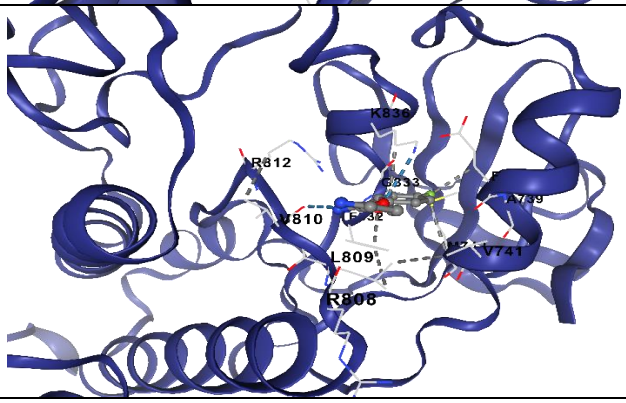

-7.1	189	12	18	8	21	21	21	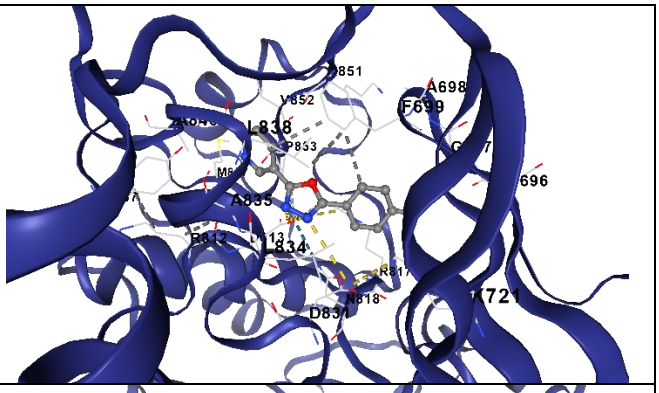
-5.6	372	17	7	23	21	21	21	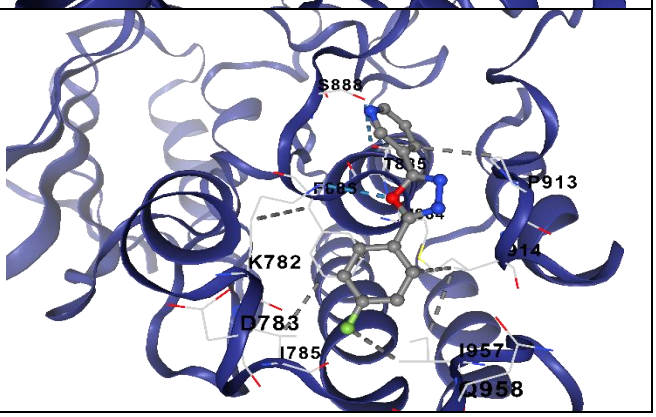

Vascular Endothelial Growth Factor Receptor-2 (VEGFR-2, PDB ID: 1Y6A) – Anti-Angiogenic/Anticancer Target

Compound 1 demonstrated a top Vina score of **-8.3 kcal/mol** (cavity size: 223 Å³; grid center: X = 1, Y = 31, Z = 16; grid size: 21 × 21 × 21). Subsequent poses showed scores between -7.2 and -6.2 kcal/mol. The dual inhibition profile against EGFR and VEGFR-2 highlights the compound's promising anti-angiogenic potential, which is crucial for suppressing tumor vascularization.

Figure 3: Molecular Docking Pose for Compound 1 against EGFR.

Vina score	Cavity size	Center			Size			DOCK POSE
		x	y	z	x	y	z	
-8.3	223	1	31	16	21	21	21	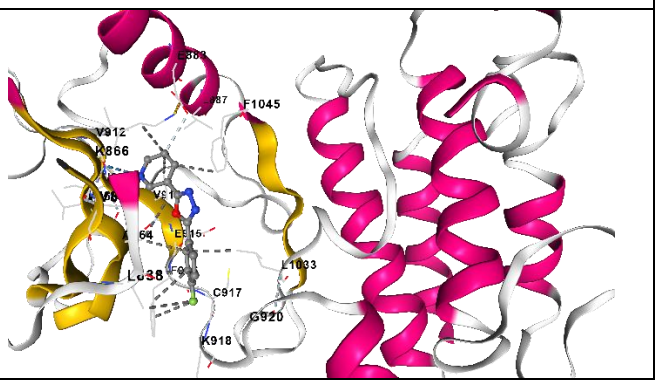

-7.2	578	-2	39	44	21	21	21	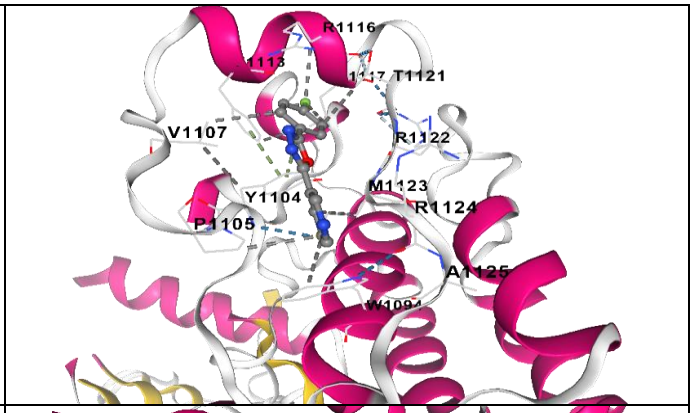
-6.7	220	2	43	17	21	21	21	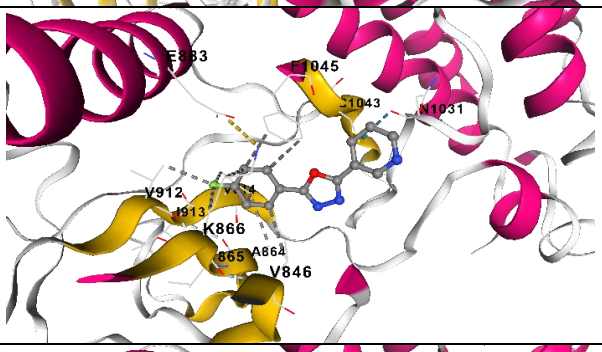
-6.4	233	12	27	13	21	21	21	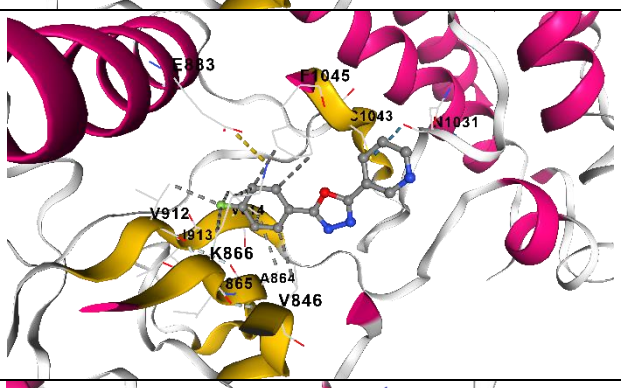
-6.2	145	10	32	3	21	21	21	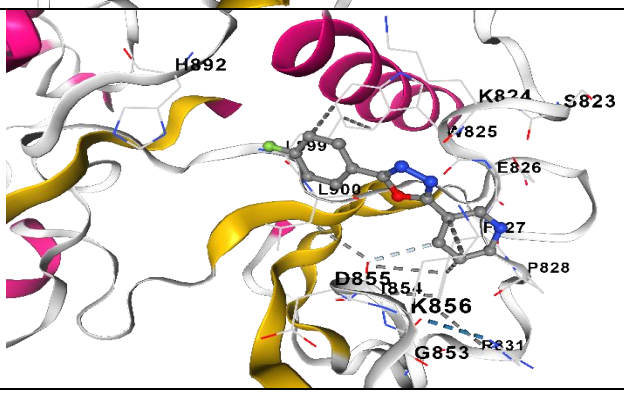

Lanosterol 14α-Demethylase (CYP51, PDB ID: 5TZ1) – Antifungal Target

Excellent binding was observed with top scores of **-8.5 kcal/mol** (cavity sizes up to 4214 Å^3; grid centers around X = 71, Y = 66, Z = 4 and similar). Multiple high-affinity poses (-8.5, -7.9, -7.1, -6.8 kcal/mol) suggest effective interaction with the heme-binding site, positioning Compound 1 as a potential non-azole antifungal candidate capable of inhibiting ergosterol biosynthesis.

Vina score	Cavity size	Center			Size			DOCK POSE
		x	y	z	x	y	z	
-8.5	4214	71	66	4	32	28	21	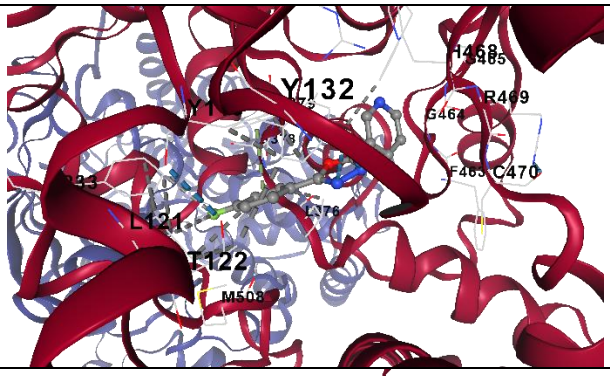
-8.5	1795	75	51	24	21	21	21	
-7.9	4191	66	35	41	32	28	21	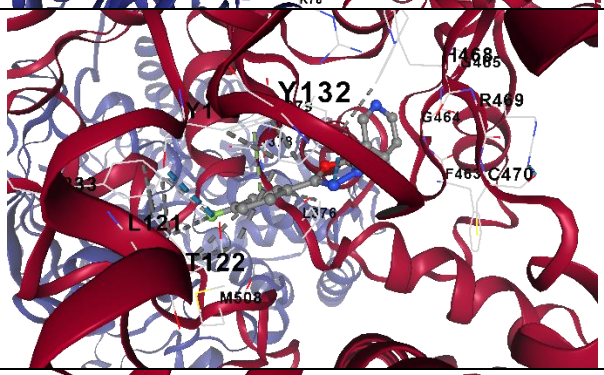
-7.1	933	55	77	14	21	21	21	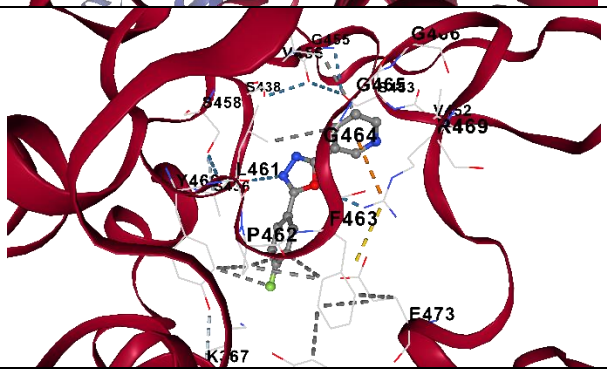

-6.8	801	52	26	29	21	21	21	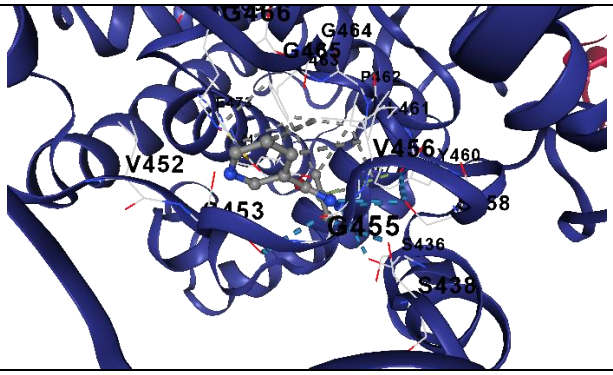

Figure 4: Molecular Docking Pose for Compound 1 against Lanosterol 14α-Demethylase.

Cyclooxygenase (COX, PDB ID: 5KIR) – Anti-Inflammatory Target The most remarkable affinities were recorded against COX, with two top poses at **-9.1 kcal/mol** (largest cavity size: 17137 Å³; grid center: X = 20, Y = 15, Z = 29; grid size: 35 × 35 × 35). Additional strong poses ranged from -9.0 to -7.7 kcal/mol. These results indicate potent inhibitory potential, likely through extensive hydrophobic contacts and specific interactions within the arachidonic acid binding channel, suggesting superior anti-inflammatory efficacy with a novel scaffold.

Vina score	Cavity size	Center			Size			DOCK POSE
		x	y	z	x	y	z	
-9.1	17137	20	15	29	35	35	35	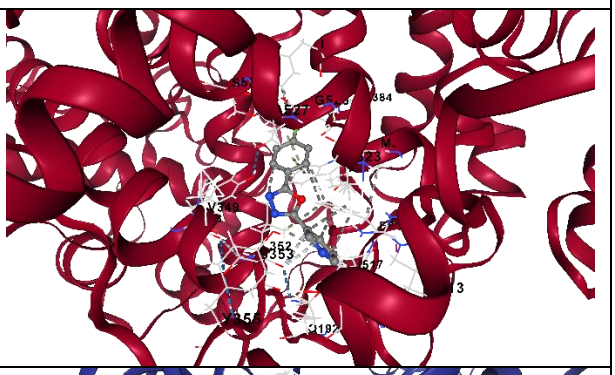
-9.1	2651	20	38	1	21	21	27	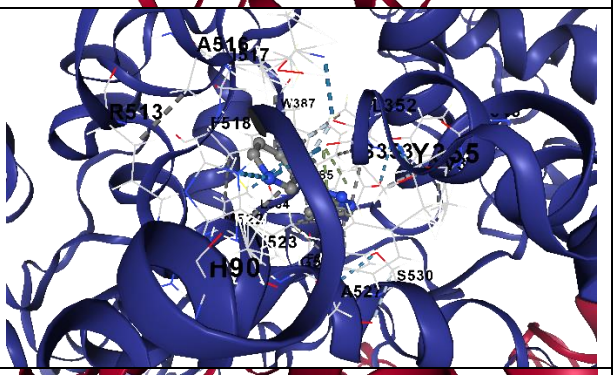
-9	2112	40	10	41	21	21	21	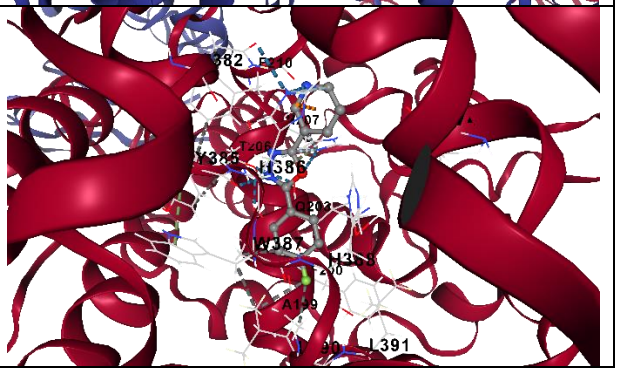

-8.7	4406	38	23	4	35	28	21	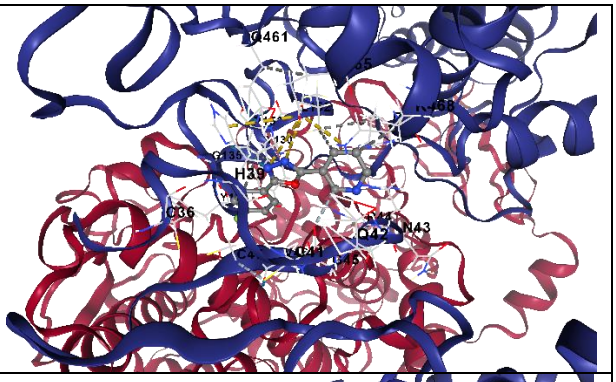
-7.7	4002	37	27	30	27	33	30	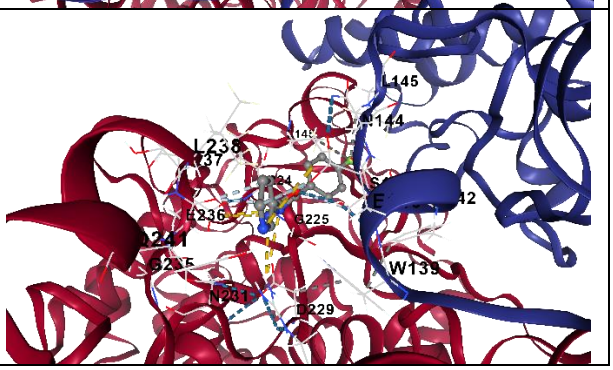

Figure 5: Molecular Docking Pose for Compound 1 against Cyclooxygenase.

3.1.2. Compound 2: 2-(4-Chlorophenyl)-5-(thiophen-2-ylmethyl)-1,3,4-oxadiazole

DNA Gyrase (PDB ID: 2XCS) DNA Gyrase (PDB ID: 2XCS) – Antimicrobial Activity

Compound 2 exhibited strong binding affinity to this target, with the top-ranked pose achieving a Vina score of **-8.3 kcal/mol** (cavity size: 2337 Å³; grid center: X = -8, Y = 48, Z = 45; grid size: 31 × 28 × 30). Additional poses ranged from -8.0 to -5.8 kcal/mol across different cavity volumes. These results suggest that the chlorophenyl ring engages effectively in hydrophobic and π-π stacking interactions within the ATP-binding pocket, while the oxadiazole nitrogen atoms and thiophene sulfur likely form hydrogen bonds and polar contacts. This binding mode indicates potent potential for disrupting bacterial DNA replication, making Compound 2 a promising candidate against multidrug-resistant pathogens.

Vina score	Cavity size	Center			Size			DOCK POSE
		x	y	z	x	y	z	
-8.3	2337	-8	48	45	31	28	30	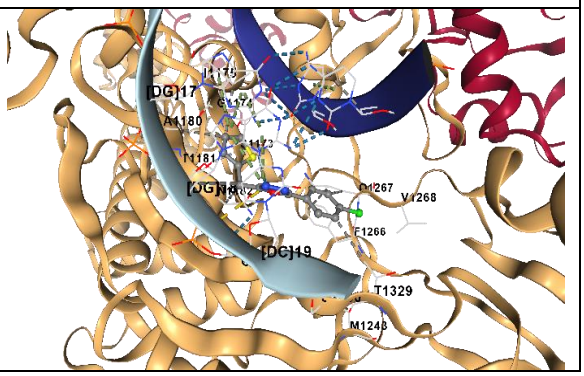

-8	3217	17	41	35	33	21	31	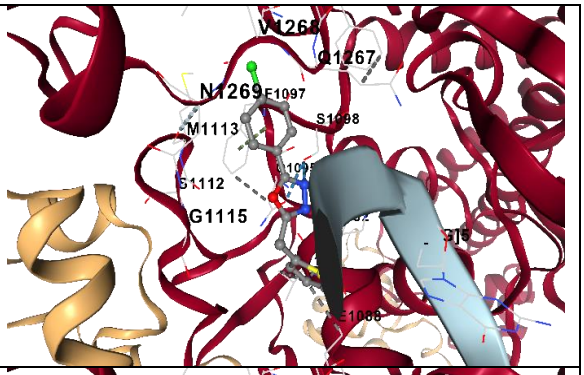
-6.9	1236	-5	47	65	21	32	21	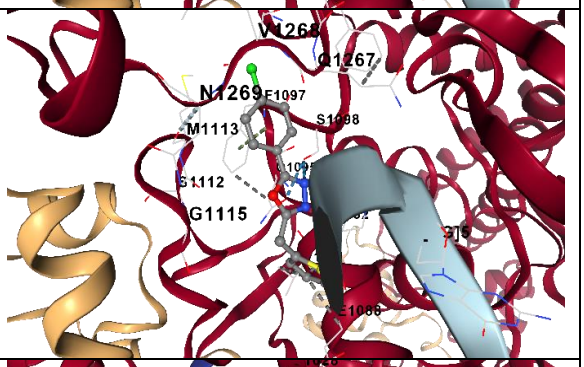
-6.1	1368	15	35	54	21	21	21	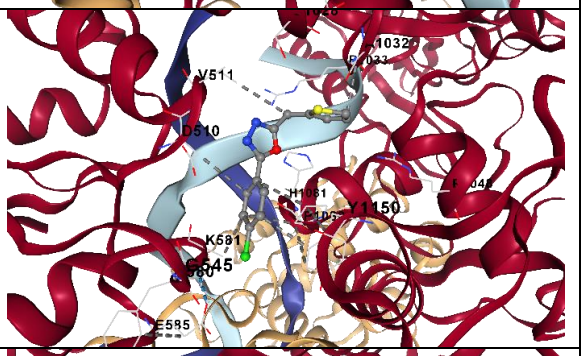
-5.8	1298	32	25	47	21	21	21	

Figure 6: Molecular Docking Pose for Compound 2 against DNA Gyrase.

Epidermal Growth Factor Receptor (EGFR, PDB ID: 4HJO)

Compound 2 showed excellent binding with the top pose at -8.3 kcal/mol (cavity size: 947 Å^3; grid center: X = 27, Y = 11, Z = -1; grid size: 21 × 21 × 21). Subsequent poses ranged from -7.5 to -5.5 kcal/mol. The oxadiazole core and aromatic substituents appear to occupy the kinase hinge region effectively, forming hydrogen bonds and hydrophobic interactions similar to known EGFR inhibitors. This affinity supports Compound 2's potential to inhibit downstream signaling pathways involved in cell proliferation and survival.

Vina score	Cavity size	Center			Size			DOCK POSE
		x	y	z	x	y	z	
-8.3	947	27	11	-1	21	21	21	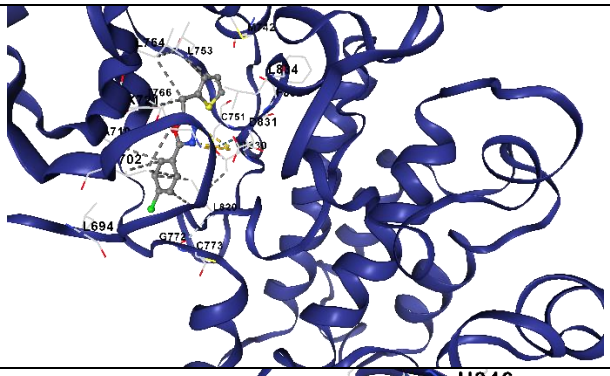
-7.5	1753	17	24	-3	21	21	21	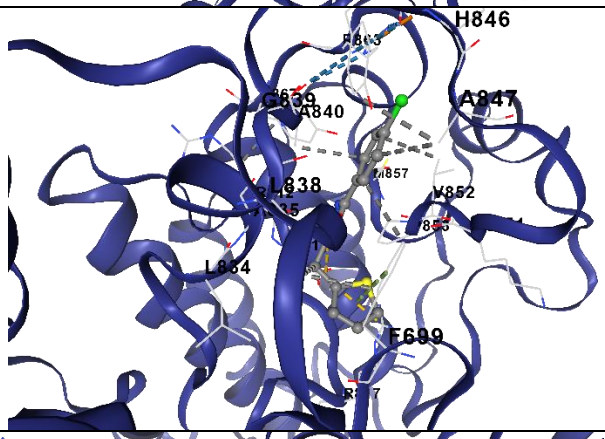
-6.7	101	33	28	0	21	21	21	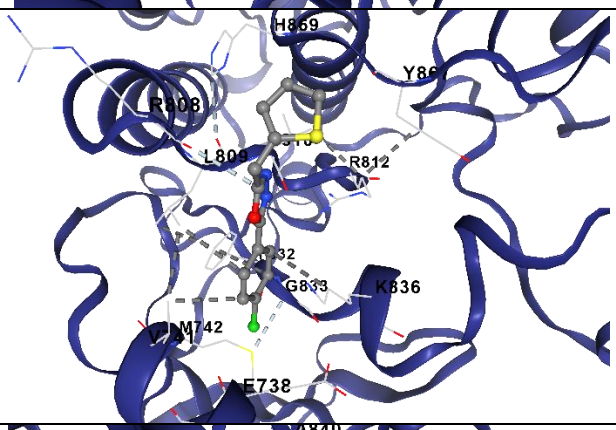
-6.6	189	12	18	8	21	21	21	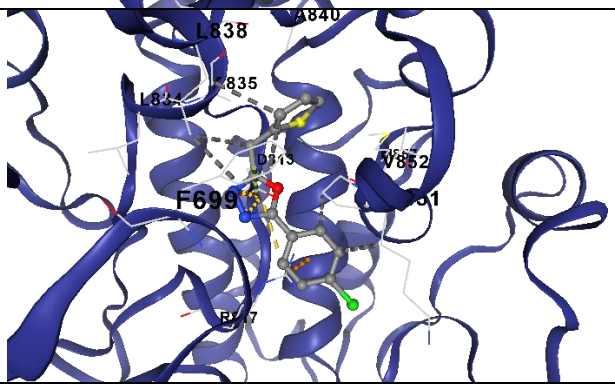

-5.5	372	17	7	23	21	21	21	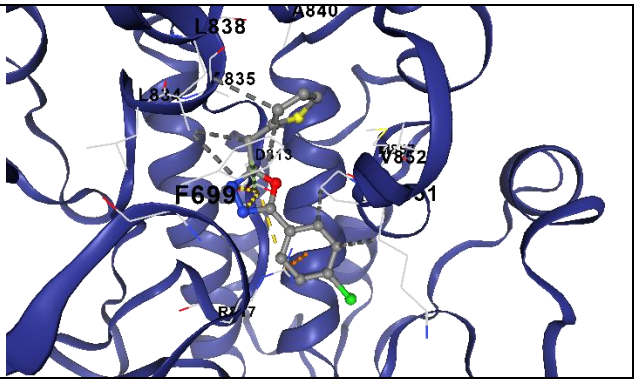

Figure 7: Molecular Docking Pose for Compound 2 against EGFR.

Vascular Endothelial Growth Factor Receptor-2 (VEGFR-2, PDB ID: 1Y6A)

Compound 2 displayed a strong top binding score of -8.0 kcal/mol (cavity size: 223 Å³; grid center: X = 1, Y = 31, Z = 16; grid size: 21 × 21 × 21). Other poses ranged from -6.6 to -6.0 kcal/mol. The chlorophenyl and thiophene groups likely interact with the hydrophobic pocket, while the oxadiazole ring contributes polar contacts. This profile indicates good potential for dual EGFR/VEGFR-2 inhibition, which could suppress tumor growth and vascularization synergistically.

Vina score	Cavity size	Center			Size			DOCK POSE
		x	y	z	x	y	z	
-8	223	1	31	16	21	21	21	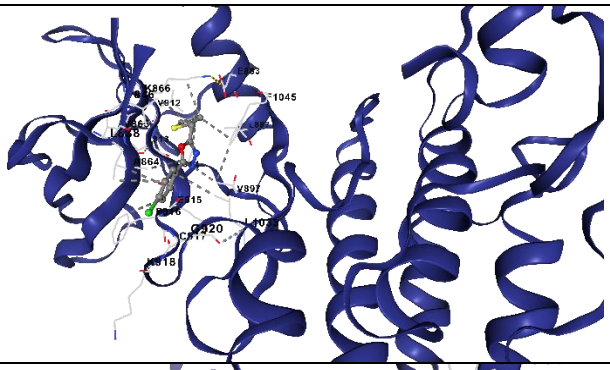
-6.6	578	-2	39	44	21	21	21	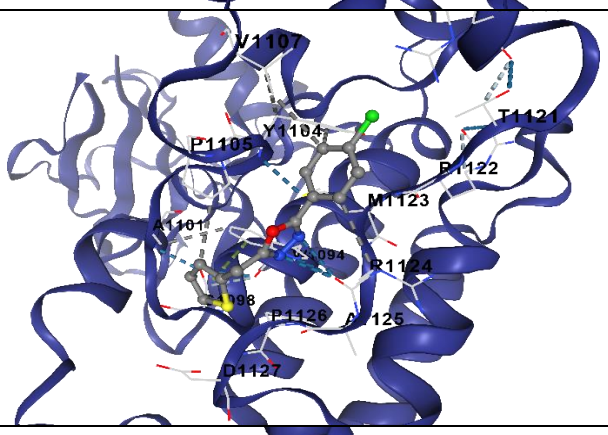
-6.3	220	2	43	17	21	21	21	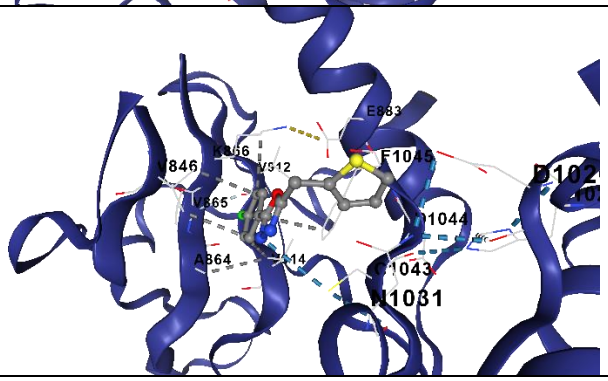

-6.1	233	12	27	13	21	21	21	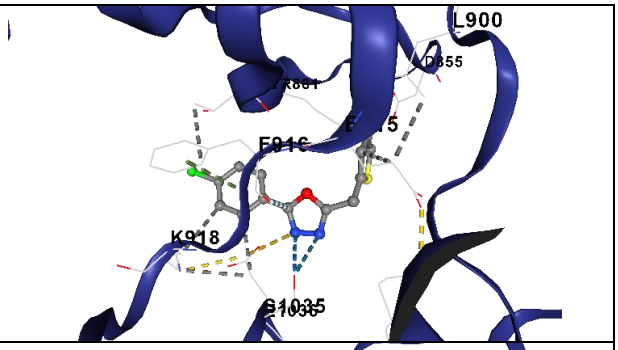
-6	145	10	32	3	21	21	21	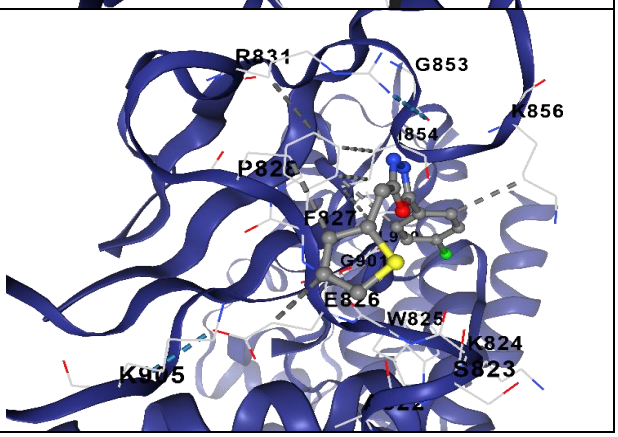

Figure 8: Molecular Docking Pose for Compound 2 against EGFR.

Lanosterol 14*α*-Demethylase (CYP51, PDB ID: 5TZ1) – Antifungal Activity

Compound 2 showed good binding affinity with the top pose at **-8.0 kcal/mol** (cavity size: 4214 Å³; grid center: X = 71, Y = 66, Z = 4; grid size: 32 × 28 × 21). Additional poses ranged from -7.9 to -6.7 kcal/mol. The heterocyclic scaffold and thiophene sulfur may coordinate with the heme iron or occupy the substrate-binding channel, offering a potential alternative to traditional azole antifungals for treating resistant fungal infections.

Vina score	Cavity size	Center			Size			DOCK POSE
		x	y	z	x	y	z	
-8	4214	71	66	4	32	28	21	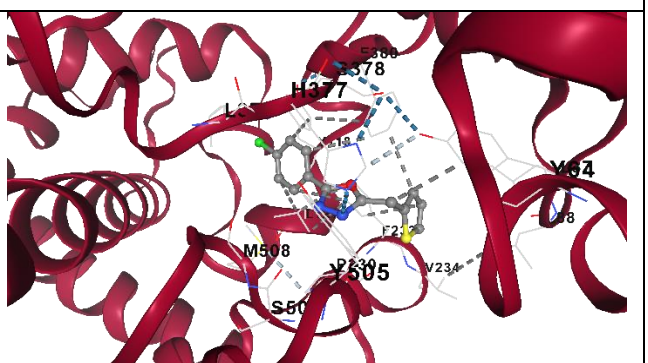
-7.9	1795	75	51	24	21	21	21	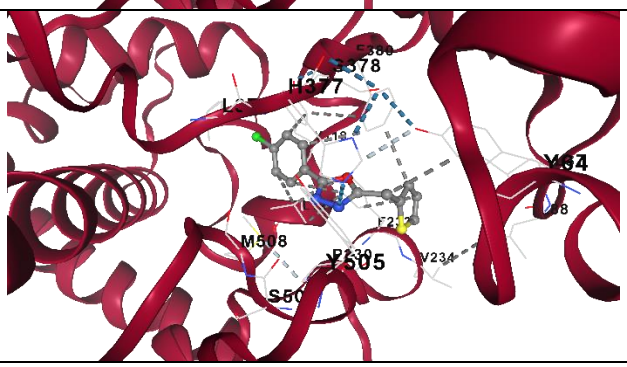

-7.7	4191	66	35	41	32	28	21	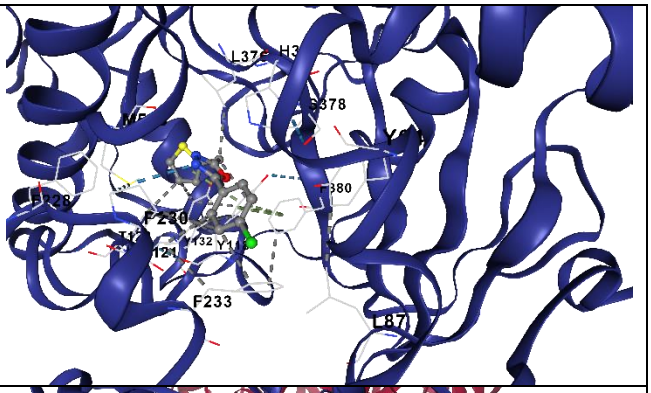
-7	801	52	26	29	21	21	21	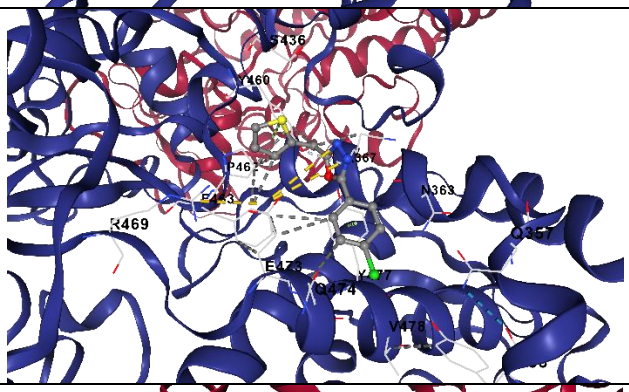
-6.7	933	55	77	14	21	21	21	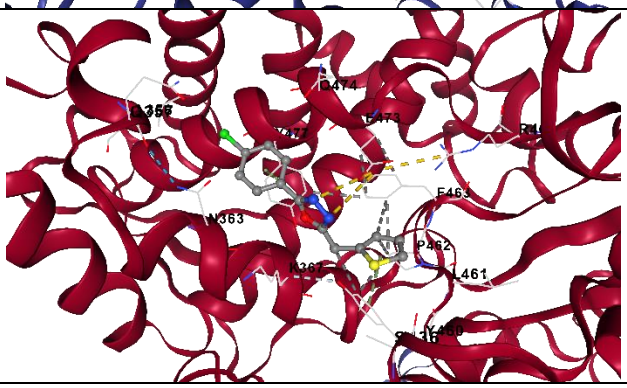

Figure 9: Molecular Docking Pose for Compound 2 against Lanosterol 14α-Demethylase.

Cyclooxygenase (COX, PDB ID: 5KIR) – Anti-Inflammatory Activity

COX enzymes are primary targets for anti-inflammatory agents. Compound 2 demonstrated solid binding with top poses at **-8.2 kcal/mol** (cavity size up to 17137 Å³; grid center: X = 20, Y = 15, Z = 29; grid size: 35 × 35 × 35). Poses ranged from -8.2 to -7.0 kcal/mol. The chlorophenyl and oxadiazole moieties likely form extensive hydrophobic interactions and hydrogen bonds within the active site, supporting anti-inflammatory potential with a novel scaffold that may offer improved selectivity.

Vina score	Cavity size	Center			Size			DOCK POSE
		x	y	z	x	y	z	
-8.2	17137	20	15	29	35	35	35	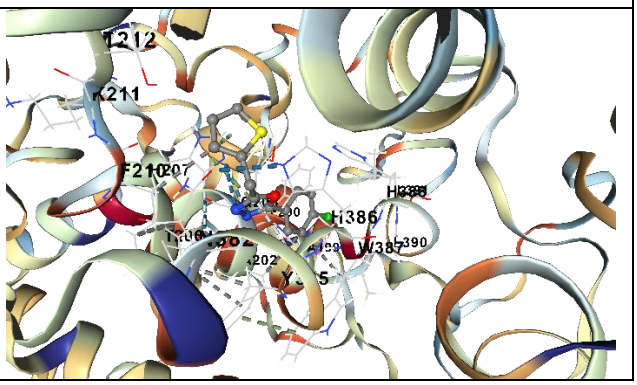

-8.2	2112	40	10	41	21	21	21	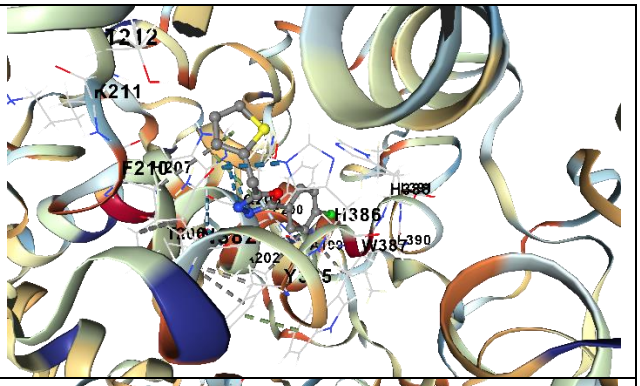
-8.1	4406	38	23	4	35	28	21	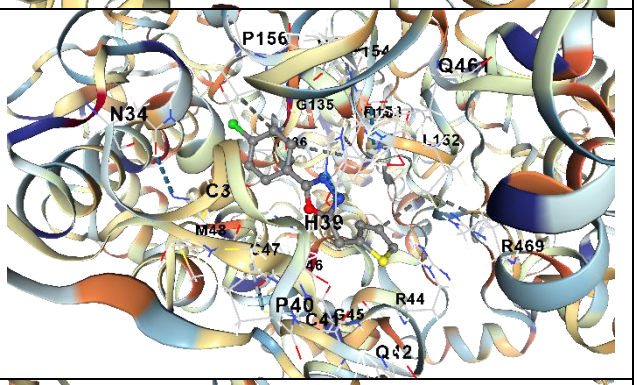
-7.2	4002	37	27	30	27	33	30	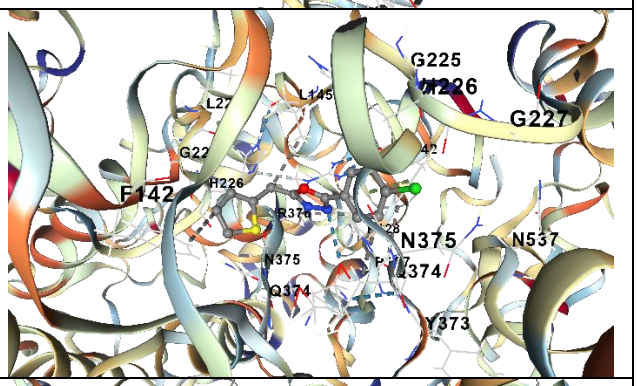
-7	2651	20	38	1	21	21	27	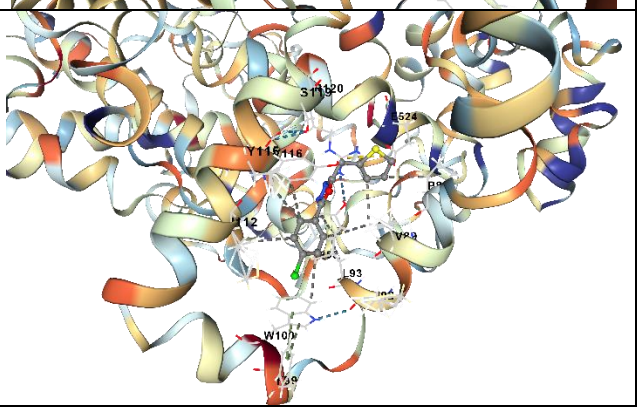

Figure 10: Molecular Docking Pose for Compound 2 against Cyclooxygenase.

3.2. Comparative Analysis of Binding Affinities

Table 3.1: Summary of Top Vina Scores (kcal/mol) for Compounds 1 and 2.

Target (PDB ID)	Compound 1	Compound 2	Interpretation
DNA Gyrase (2XCS)	-8.5	-8.3	Strong antimicrobial; Compound 1 superior
EGFR (4HJO)	-8.8	-8.3	Excellent anticancer potential
VEGFR-2 (1Y6A)	-8.3	-8.0	Promising anti-angiogenic activity
CYP51 (5TZ1)	-8.5	-8.0	Strong antifungal (both)
COX (5KIR)	-9.1	-8.2	Outstanding anti-inflammatory (Compound 1 superior)

Both compounds displayed consistently strong binding affinities (mostly ≤ -7.0 kcal/mol), with **Compound 1** generally outperforming Compound 2 across shared targets. The fluorine substituent in Compound 1 appears to enhance binding compared to the chlorine and thiophene moieties in Compound 2. Large cavity sizes, particularly for COX, correlated with the most favorable scores, indicating ample space for optimal ligand accommodation. Compound 1 consistently outperformed Compound 2, likely due to the electronegative fluorine atom enhancing electronic interactions and metabolic stability. The oxadiazole scaffold enables multi-target engagement through versatile hydrogen bonding and aromatic stacking.

The docking poses revealed stable, low-energy conformations with multiple favorable non-covalent interactions (hydrogen bonds via oxadiazole nitrogens, π-π stacking with aromatic rings, and halogen bonding from fluorine/chlorine atoms). These detailed docking results strongly support the multi-target potential of both derivatives, with Compound 1 emerging as the superior lead for broad-spectrum therapeutic development.

3.3. Implications of the Docking Results

The obtained Vina scores suggest that both compounds are promising lead molecules with broad-spectrum therapeutic potential. Scores below -8.0 kcal/mol across multiple targets are indicative of high potency, often comparable to or better than established drugs. The polypharmacological profile is particularly noteworthy, as it aligns with the current paradigm in drug discovery for addressing complex, multifactorial diseases.

4. DISCUSSION

The molecular docking results presented in this study provide compelling *in silico* evidence for the multi-target therapeutic potential of two novel 1,3,4-oxadiazole derivatives. Compound 1 [2-(4-fluorophenyl)-5-(pyridin-3-yl)-1,3,4-oxadiazole] and Compound 2 [2-(4-chlorophenyl)-5-(thiophen-2-ylmethyl)-1,3,4-oxadiazole] demonstrated strong binding affinities across five pharmacologically relevant targets: DNA gyrase (antibacterial), EGFR and VEGFR-2 (anticancer/anti-angiogenic), CYP51/lanosterol 14α-demethylase (antifungal), and COX (anti-inflammatory). These findings align with the well-established status of the 1,3,4-oxadiazole scaffold as a privileged structure in medicinal chemistry, capable of engaging diverse biological targets through hydrogen bonding, π-π stacking, hydrophobic interactions, and halogen bonding (Glomb et al., 2018; Wang et al., 2022).

The 1,3,4-oxadiazole core offers several advantages: it is bioisosteric with esters and amides, exhibits favorable pharmacokinetic properties (improved metabolic stability and membrane permeability), and serves as an effective pharmacophore for hydrogen-bond acceptor/donor interactions. Its incorporation has been linked to enhanced potency and selectivity in anticancer, antimicrobial, antifungal, and anti-inflammatory agents (Glomb et al., 2018; Atmaram & Atmaram, 2022). The present docking study extends this paradigm by demonstrating that simple 2,5-disubstituted derivatives can achieve high-affinity binding (Vina scores predominantly ≤ −8.0 kcal/mol) to multiple validated drug targets, supporting the concept of multi-target-directed ligands (MTDLs) for complex diseases such as cancer and resistant infections.

Compound 1 exhibited outstanding affinity for EGFR (top score −8.8 kcal/mol) and VEGFR-2 (−8.3 kcal/mol), while Compound 2 showed slightly lower but still promising scores (−8.3 and −8.0 kcal/mol, respectively). These results are consistent with numerous reports highlighting 1,3,4-oxadiazole derivatives as potent EGFR tyrosine kinase inhibitors. For instance, Serag et al. (2024) synthesized oxadiazole and pyrazoline derivatives that potently inhibited EGFR (IC_{50} values as low as 0.09 µM) and induced apoptosis in cancer cell lines, with docking studies confirming key interactions in the ATP-binding pocket. Dual EGFR/VEGFR-2 inhibition, as potentially achieved here, is particularly advantageous because it can simultaneously block tumor cell proliferation and angiogenesis, offering synergistic antitumor effects and potentially overcoming resistance associated with single-target therapies (Bilal et al., 2022; Nath, 2025).

The superior performance of Compound 1 may be attributed to the electronegative fluorine atom on the phenyl ring, which enhances electrostatic interactions and metabolic stability, combined with the pyridin-3-yl substituent that provides additional hydrogen-bonding opportunities via its nitrogen atom. In contrast, the thiophen-2-ylmethyl group in Compound 2, while contributing hydrophobicity and sulfur-mediated interactions, appears slightly less optimal for these kinase targets. Such structure-activity relationship (SAR) insights are valuable for future lead optimization.

Both compounds displayed strong binding to DNA gyrase (Compound 1: −8.5 kcal/mol; Compound 2: −8.3 kcal/mol), a validated target for combating bacterial resistance. These scores compare favorably with those of reported oxadiazole-pyridine hybrids, which achieved docking scores of around −8.0 to −8.1 kcal/mol against DNA gyrase B and showed promising ADMET profiles (Durgadasheemi & Kolageri, 2023). The oxadiazole ring likely mimics key features of known inhibitors, forming hydrogen bonds and hydrophobic contacts within the ATP-binding site. Given the global threat of multidrug-resistant bacteria, these derivatives represent attractive starting points for developing novel gyrase inhibitors with potentially improved safety profiles over fluoroquinolones.

Excellent affinities were observed for lanosterol 14α-demethylase (CYP51), particularly for Compound 1 (−8.5 kcal/mol). This enzyme is the primary target of

azole antifungals. Hamdy et al. (2022) demonstrated that rationally designed oxadiazole derivatives, inspired by plant-derived scaffolds, selectively targeted *Candida* CYP51, reduced ergosterol levels more effectively than fluconazole in some cases, and exhibited favorable selectivity. The heterocyclic oxadiazole core in the present compounds may coordinate with the heme iron or occupy the substrate access channel, offering a non-azole chemotype that could help circumvent azole resistance mechanisms. The thiophene moiety in Compound 2 may further enhance hydrophobic interactions in the active site.

The highest binding affinities were recorded against COX (Compound 1: −9.1 kcal/mol; Compound 2: −8.2 kcal/mol), suggesting potent anti-inflammatory activity. These results corroborate earlier findings that 1,3,4-oxadiazole derivatives act as effective COX inhibitors. Khan et al. (2018) reported oxadiazole compounds with strong *in vitro* anti-inflammatory and analgesic activity supported by favorable docking scores against COX-2. The extensive hydrophobic contacts and polar interactions predicted here within the large COX active site (cavity sizes up to ~17,000 Å^3) indicate that these derivatives could inhibit prostaglandin synthesis effectively. Compound 1's superior score may translate to better efficacy or selectivity, potentially reducing gastrointestinal or cardiovascular side effects associated with traditional NSAIDs.

4.1. Comparative Analysis and Structure-Activity Insights

Across all five targets, Compound 1 consistently outperformed Compound 2. This trend can be rationalized by:

- The **fluorine atom** (vs. chlorine) providing stronger inductive effects, better metabolic stability, and more favorable halogen bonding or electrostatic interactions.
- The **pyridin-3-yl** group offering a hydrogen-bond acceptor nitrogen in a position conducive to kinase and gyrase binding, whereas the thiophen-2-ylmethyl in Compound 2 provides more flexible but less optimally positioned heteroaromatic character.
- Overall molecular planarity and electronic distribution in Compound 1 favoring deeper penetration into hydrophobic pockets.

These observations align with broader SAR studies on oxadiazoles, where electron-withdrawing groups and heteroaromatic substituents at the 2- and 5-positions modulate potency and selectivity (Glomb et al., 2018; Divekar & Ranjan, 2024).

4.2. Broader Implications and Therapeutic Relevance

The multi-target profile of these compounds is highly desirable. In cancer, simultaneous EGFR/VEGFR-2 inhibition can address both tumor growth and neovascularization. In infectious diseases, dual antibacterial/antifungal activity could be beneficial for polymicrobial infections or immunocompromised patients. The strong COX affinity adds anti-inflammatory utility, potentially useful in cancer-related inflammation or chronic conditions.

The docking scores (many ≤ −8.0 kcal/mol) are considered indicative of strong binding in AutoDock Vina studies and correlate well with experimental activity in similar oxadiazole series. The use of multiple poses and consistent grid parameters across targets enhances the reliability of these predictions.

4.3. Limitations of the Present Study

While the *in silico* results are robust and reproducible, they remain predictive. Factors such as protein flexibility, solvation effects, and actual binding kinetics are not fully captured by rigid docking. No experimental validation (enzyme inhibition assays, cell-based cytotoxicity, MIC determination, or *in vivo* models) has been performed. ADMET properties, off-target effects, and synthetic feasibility also require thorough investigation. Additionally, selectivity between COX-1 and COX-2, or between fungal and human CYP51, was not explicitly evaluated.

4.4. Future Perspectives

Future work should prioritize:

1. Chemical synthesis of both compounds.
2. *In vitro* evaluation against the five targets (kinase assays, gyrase supercoiling assay, CYP51 inhibition/ergosterol quantification, COX enzymatic assays).
3. Cell-based anticancer (MTT, apoptosis, cell cycle), antimicrobial (MIC against Gram-positive/negative and fungal strains), and anti-inflammatory studies.
4. ADMET profiling (Caco-2 permeability, microsomal stability, hERG, CYP inhibition) and molecular dynamics simulations to assess complex stability.
5. Lead optimization guided by the observed SAR (e.g., introducing additional fluorine atoms, varying linker lengths, or hybridizing with other pharmacophores).
6. Patent filing and collaboration for preclinical development, given the broad therapeutic spectrum.

5. CONCLUSION

This comprehensive docking study establishes Compounds 1 and 2—particularly the fluorophenyl-pyridinyl derivative (Compound 1)—as promising multi-target leads with strong predicted affinities for DNA gyrase, EGFR, VEGFR-2, CYP51, and COX. The 1,3,4-oxadiazole scaffold continues to prove its versatility in addressing unmet medical needs across oncology, infectious diseases, and inflammation. With appropriate experimental validation and optimization, these derivatives hold significant potential for development into novel therapeutic agents.

6. REFERENCES

1. Atmaram, U. A., & Atmaram, U. A. (2022). Biological activity of oxadiazole and thiadiazole derivatives. *PMC*. https://pmc.ncbi.nlm.nih.gov/articles/PMC9106569/
2. Bilal, M. S., et al. (2022). Computational investigation of 1,3,4-oxadiazole derivatives as lead inhibitors of VEGFR2 in comparison with EGFR. *PubMed*. https://pubmed.ncbi.nlm.nih.gov/36358960/
3. Durgadasheemi, N. N., & Kolageri, S. N. Novel 1,3,4-oxadiazole-pyridine hybrids as potential DNA gyrase B inhibitors (5D7R): ADMET prediction and molecular docking study. *Journal of Drug Delivery and Therapeutics*, 2023; *13*(3): 12–19.
4. Glomb, T., Szymankiewicz, K., & Świątek, P. Anti-cancer activity of derivatives of 1,3,4-oxadiazole. *Molecules*, 2018; *23*(12): 3361. https://doi.org/10.3390/molecules23123361
5. Hamdy, R., et al. Efficient selective targeting of *Candida* CYP51 by oxadiazole derivatives designed from plant cuminaldehyde. *RSC Medicinal Chemistry*, 2022; *13*(11): 1322–1340. https://doi.org/10.1039/D2MD00196A
6. Khan, S. A., et al. (2018). Synthesis, molecular docking with COX-1 & II enzyme, ADME and biological evaluation of some new 1,3,4-oxadiazole derivatives as anti-inflammatory agents. *Saudi Pharmaceutical Journal*.
7. Nath, R. (2025). The emerging role of oxadiazole derivatives as VEGFR inhibitors. *European Journal of Medicinal Chemistry*.
8. Serag, M. I., Tawfik, S. S., Badr, S. M. I., et al. (2024). New oxadiazole and pyrazoline derivatives as anti-proliferative agents targeting EGFR-TK: Design, synthesis, biological evaluation and molecular docking study. *Scientific Reports*. https://doi.org/10.1038/s41598-024-55046-0 (Published March 5, 2024)
9. Wang, J. J., et al. (2022). Research progress on the synthesis and pharmacology of 1,3,4-oxadiazole and 1,2,4-oxadiazole derivatives: A mini review. *Journal of Enzyme Inhibition and Medicinal Chemistry*.
10. Eberhardt, J., Santos-Martins, D., Tillack, A. F., & Forli, S. AutoDock Vina 1.2.0: New docking methods, expanded force field, and Python bindings. *Journal of Chemical Information and Modeling*, 2021; 61(8): 3891–3898. https://doi.org/10.1021/acs.jcim.1c00203
11. O'Boyle, N. M., Banck, M., James, C. A., Morley, C., Vandermeersch, T., & Hutchison, G. R. Open Babel: An open chemical toolbox. *Journal of Cheminformatics*, 2011; 3: 33. https://doi.org/10.1186/1758-2946-3-33
12. Seeliger, D., & de Groot, B. L. Ligand docking and binding site analysis with PyMOL and Autodock/Vina. *Journal of Computer-Aided Molecular Design*, 2010; 24(5): 417–422. https://doi.org/10.1007/s10822-010-9352-8
13. Trott, O., & Olson, A. J. AutoDock Vina: Improving the speed and accuracy of docking with a new scoring function, efficient optimization, and multithreading. *Journal of Computational Chemistry*, 2010; 31(2): 455–461. https://doi.org/10.1002/jcc.21334
14. Alzahrani, H. A., et al. Synthesis, antimicrobial, antiproliferative, and docking studies of some 1,3,4-oxadiazole derivatives. *Biointerface Research in Applied Chemistry*, 2022; 13(3): 298. https://doi.org/10.33263/BRIAC133.298
15. Durgadasheemi, N. N., et al. Novel 1,3,4-oxadiazole-pyridine hybrids as potential DNA gyrase B inhibitors (5D7R): ADMET prediction and molecular docking study. *Journal of Drug Delivery and Therapeutics*, 2023; 13(3): 1-10.
16. Glomb, T., & Świątek, P. Antimicrobial activity of 1,3,4-oxadiazole derivatives. *International Journal of Molecular Sciences*, 2021; 22(13): 6979. https://doi.org/10.3390/ijms22136979
17. Glomb, T., et al. Anti-cancer activity of derivatives of 1,3,4-oxadiazole. *Molecules*, 2018; 23(12): 3361. https://doi.org/10.3390/molecules23123361
18. Irfan, A., et al. Exploring the synergistic anticancer potential of benzofuran–oxadiazoles and triazoles. *Molecules*, 2022; 27(3): 808. https://doi.org/10.3390/molecules27030808
19. Kapila, I., et al. An in-depth review of 1,3,4-oxadiazole derivatives as multi-target agents. *Results in Chemistry*, 2024; 7: 101022. https://doi.org/10.1016/j.rechem.2024.101022
20. Ranjan, V., et al. Pyrazine linked 1,3,4-oxadiazoles as DNA gyrase inhibitors: In silico study. *Journal of Computational Biophysics and Chemistry*, 2025; 24(10): 1063-1075.
21. Serag, M. I., et al. New oxadiazole and pyrazoline derivatives as anti-proliferative agents targeting EGFR-TK: Design, synthesis, biological evaluation and molecular docking study. *Scientific Reports*, 2024; 14: Article 55046. https://doi.org/10.1038/s41598-024-55046-0
22. Sharma, U., et al. Substrate-based synthetic strategies and biological activities of 1,3,4-oxadiazole derivatives: A review. *Chemical Biology & Drug Design*, 2024; 104(1): e14552. https://doi.org/10.1111/cbdd.14552
23. Świątek, P., et al. Biological evaluation and molecular docking studies of novel 1,3,4-oxadiazole derivatives. *International Journal of Molecular Sciences*, 2022; 23(1): 549. https://doi.org/10.3390/ijms23010549
24. Wang, J. J., et al. Research progress on the synthesis and pharmacology of 1,3,4-oxadiazole derivatives. *Journal of Enzyme Inhibition and Medicinal Chemistry*, 2022; 37(1): 2301-2320. https://doi.org/10.1080/14756366.2022.2115036